

# LINC-PINT Suppresses the Aggressiveness of Thyroid Cancer by Downregulating miR-767-5p to Induce TET2 Expression

Meng Jia,<sup>1</sup> Zhuyao Li,<sup>1</sup> Mengjiao Pan,<sup>1</sup> Mei Tao,<sup>1</sup> Jiaxiang Wang,<sup>2</sup> and Xiubo Lu<sup>1</sup>

<sup>1</sup>Department of Thyroid Surgery, The First Affiliated Hospital of Zhengzhou University, Zhengzhou, Henan 450052, China; <sup>2</sup>Department of Pediatric Surgery, The First Affiliated Hospital of Zhengzhou University, Zhengzhou, Henan 450052, China

**Long noncoding RNA (lncRNA) long intergenic nonprotein-coding RNA, p53-induced transcript (LINC-PINT) has shown anti-invasive activity in lung and colon cancer cells. However, the role of LINC-PINT in thyroid cancer is unclear. In the present work, we explored the expression of LINC-PINT in 60 paired thyroid cancer and adjacent normal tissues. The clinical significance and biological function of LINC-PINT in thyroid cancer were determined. LINC-PINT expression was downregulated in thyroid cancer relative to adjacent normal tissues ( $p = 0.0002$ ). Low expression of LINC-PINT was significantly associated with advanced tumor node metastasis (TNM) stage ( $p = 0.0306$ ) and lymph node metastasis ( $p = 0.0359$ ). Ectopic expression of LINC-PINT suppressed the proliferation, invasion, and tumorigenesis of thyroid cancer cells. Mechanistically, LINC-PINT associated with and downregulated microRNA (miR)-767-5p. Moreover, LINC-PINT overexpression relieved miR-767-5p-mediated repression of ten-eleven translocation 2 (TET2). miR-767-5p promoted aggressiveness of thyroid cancer, which was reversed by overexpression of TET2. Coexpression of miR-767-5p or depletion of TET2 rescued the inhibitory effect of LINC-PINT on thyroid cancer cell proliferation and invasion. In addition, there was a negative correlation between miR-767-5p and LINC-PINT in thyroid cancer ( $r = -0.34772$ ,  $p = 0.01789$ ). Taken together, LINC-PINT functions as a tumor suppressor in thyroid cancer via the miR-767-5p/TET2 axis, representing a potential therapeutic target for thyroid cancer.**

## INTRODUCTION

Thyroid cancer is the most commonly diagnosed malignancy of the endocrine system.<sup>1,2</sup> Thyroid cancer can be classified as papillary thyroid cancer (PTC), follicular thyroid cancer (FTC), anaplastic thyroid cancer (ATC), and medullary thyroid cancer (MTC). PTC is the major subtype, accounting for 80% of thyroid cancers.<sup>3</sup> Although well-differentiated thyroid cancers have an overall good prognosis, some of them can progress to an aggressive, lethal disease.<sup>4,5</sup> The understanding of the molecular basis of thyroid cancer progression is critical for development of effective targeted therapies.

The ten-eleven translocation (TET) family comprising three members (TET1, TET2, and TET3) is an important epigenetic modifier.<sup>6</sup> TET

proteins are capable of converting 5-methyl-cytosine (5-mC) to 5-hydroxymethyl-cytosine (5-hmC), consequently leading to DNA demethylation.<sup>7</sup> Accumulating evidence has linked TET proteins to tumorigenesis.<sup>8,9</sup> For instance, Zhou et al.<sup>9</sup> reported that knockdown of TET1 facilitates colon cancer cell migration and invasion. Both TET1 and TET2 are deregulated in thyroid cancer.<sup>8,10</sup> These results suggest an involvement of TETs in thyroid cancer progression.

Long noncoding RNAs (lncRNAs) are a large family of endogenous RNAs of >200 nt in length without protein-coding capacity.<sup>11</sup> They participate in a wide range of physiological and pathological processes, such as development, immunity, inflammation, and carcinogenesis.<sup>12,13</sup> Interaction with microRNAs (miRNAs), which are a class of small, regulatory, noncoding RNAs,<sup>14</sup> represents an important mechanism mediating lncRNA function. For instance, Wang et al.<sup>15</sup> reported that lncRNA differentiation antagonizing nonprotein-coding RNA (DNACR) enhances the growth and lung metastasis of osteosarcoma by decoying both microRNA (miR)-335-5p and miR-1972. Similarly, Ding et al.<sup>16</sup> demonstrated that lncRNA homeobox transcript antisense intergenic RNA (HOTAIR) stimulates renal cell carcinoma cell proliferation and invasion via antagonizing multiple miRNAs, including miR-138, miR-200c, miR-204, and miR-217. Recent studies have shown that the lncRNA long intergenic nonprotein-coding RNA, p53-induced transcript (LINC-PINT) is downregulated in several cancers, including colon cancer, lung cancer, breast cancer, glioblastoma, and gastric cancer, and exhibits an anti-invasive activity.<sup>17,18</sup> However, the role of LINC-PINT in thyroid cancer progression is poorly understood.

Therefore, in this work, we aimed to explore the expression pattern, clinical significance, and function of LINC-PINT in thyroid cancer. The miRNA partner mediating the action of LINC-PINT was further characterized.

Received 17 February 2020; accepted 28 May 2020;  
<https://doi.org/10.1016/j.omtn.2020.05.033>.

**Correspondence:** Xiubo Lu, The First Affiliated Hospital of Zhengzhou University, Zhengzhou, Henan 450052, China.

**E-mail:** [doctorluxiubo@126.com](mailto:doctorluxiubo@126.com)

**Correspondence:** Jiaxiang Wang, The First Affiliated Hospital of Zhengzhou University, Zhengzhou, Henan 450052, China.

**E-mail:** [wjiaxiang@zzu.edu.cn](mailto:wjiaxiang@zzu.edu.cn)



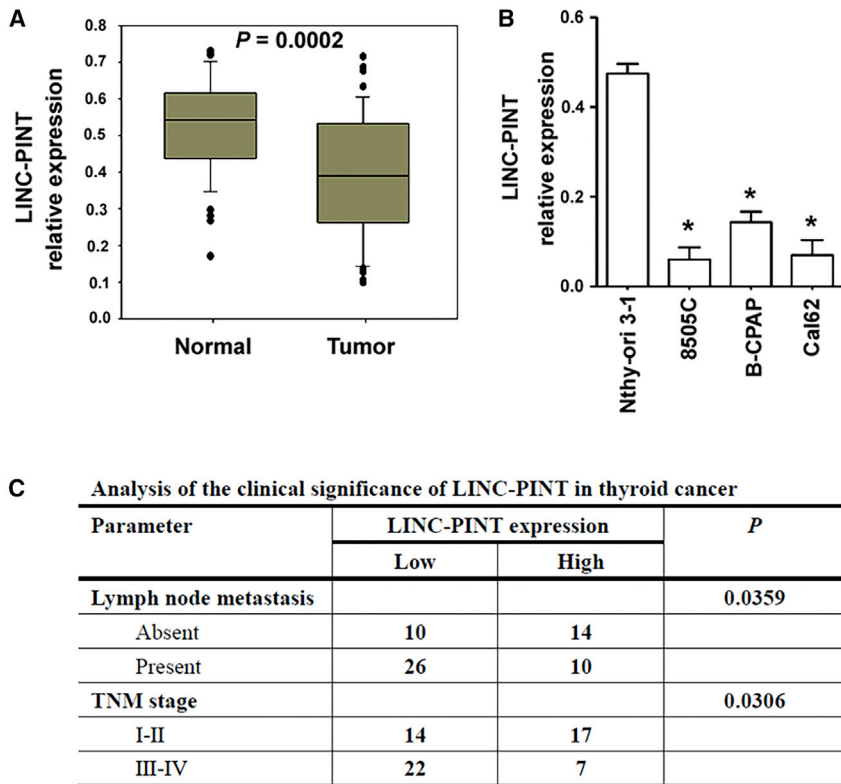


**Figure 1. Expression and Clinical Significance of LINC-PINT in Thyroid Cancer**

(A) LINC-PINT expression in 60 paired thyroid cancer and adjacent normal tissue samples. (B) LINC-PINT expression in thyroid cancer cell lines. \* $p < 0.05$  versus Nthy-ori 3-1 cells. (C) The correlations between LINC-PINT expression level and clinicopathologic parameters of patients with thyroid cancer.

in LINC-PINT-transfected cells relative to vector-transfected cells (Figure 2A). Notably, ectopic expression of LINC-PINT resulted in a significant inhibition of thyroid cancer cell proliferation (Figure 2B) and colony formation (Figure 2C). A highly invasive cell line 8505C was used in Transwell invasion assay. We found that the invasiveness of 8505C was dramatically reduced by overexpression of LINC-PINT (Figure 2D). Xenograft tumors formed by LINC-PINT-overexpressing 8505C and Cal62 cells grew significantly slower than those by vector-transfected control cells (Figures 3A and 3B). The tumor weight was reduced in the LINC-PINT group compared to the control group (Figure 3C). Immunohistochemistry staining of Ki-67 in the xenograft tumors further demonstrated a decrease of Ki-67-positive cells by LINC-PINT overexpression (Figure 3D). Taken together, LINC-PINT suppresses the growth and invasive properties of thyroid cancer cells.

#### LINC-PINT Interacts with and Downregulates miR-767-5p

To decipher the mechanism by which LINC-PINT exerts suppressive effects on the aggressiveness of thyroid cancer, we sought to search for potential target miRNAs of LINC-PINT using miRNA qPCR arrays. Among the 84 cancer-related miRNAs tested, 6 showed differential expression (>4-fold) between LINC-PINT-overexpressing 8505C and control cells (Table S1). Real-time PCR analysis further validated that miR-767-5p expression was downregulated in 8505C, B-CPAP, and Cal62 cells after LINC-PINT overexpression (Figure 4A). However, the other 5 candidate miRNAs were unaffected by LINC-PINT overexpression (data not shown). These results suggest miR-767-5p as a main miRNA mediating the action of LINC-PINT in thyroid cancer.

Compared to Nthy-ori 3-1 cells, 8505C, B-CPAP, and Cal62 thyroid cancer cell lines had increased levels of miR-767-5p (Figure 4B). Spearman's correlation analysis revealed a negative correlation between miR-767-5p and LINC-PINT in thyroid cancer tissues ( $r = -0.34772$ ,  $p = 0.01789$ ; Figure 4C). To confirm the interaction between miR-767-5p and LINC-PINT in thyroid cancer cells, we performed an anti-argonaute 2 (Ago2) RNA immunoprecipitation (RIP) assay. The results showed that both miR-767-5p and LINC-PINT were enriched in Ago2 RIP samples from 8505C and Cal62 cells (Figure 4D). Dual-luciferase reporter assay demonstrated that the LINC-PINT reporter activity

## RESULTS

### Clinical Significance of LINC-PINT in Thyroid Cancer

To explore the expression and clinical relevance of LINC-PINT in thyroid cancer, we examined its expression in 60 pairs of thyroid cancer and adjacent normal tissues. Compared to corresponding noncancerous tissues, LINC-PINT expression was downregulated in thyroid cancer tissues ( $p = 0.0002$ ; Figure 1A). Consistently, LINC-PINT levels were significantly lower in the 3 thyroid cancer cell lines (8505C, B-CPAP, and Cal62) than that in an immortalized thyroid epithelial cell line, Nthy-ori 3-1 (Figure 1B). These results indicate the downregulation of LINC-PINT in thyroid cancer tissues and cell lines.

Next, we analyzed the clinical significance of LINC-PINT in thyroid cancer. As shown in Figure 1C, low expression of LINC-PINT was significantly associated with advanced TNM stage ( $p = 0.0306$ ) and lymph node metastasis ( $p = 0.0359$ ). However, the expression level of LINC-PINT did not differ among histological subtypes of thyroid cancer (data not shown). These data indicate that LINC-PINT downregulation is linked to the progression of thyroid cancer.

### LINC-PINT Overexpression Suppresses the Proliferation, Invasion, and Tumorigenesis of Thyroid Cancer Cells

To uncover the biological function of LINC-PINT in thyroid cancer, we overexpressed LINC-PINT in 8505C, B-CPAP, and Cal62 cells. Real-time PCR analysis validated the overexpression of LINC-PINT

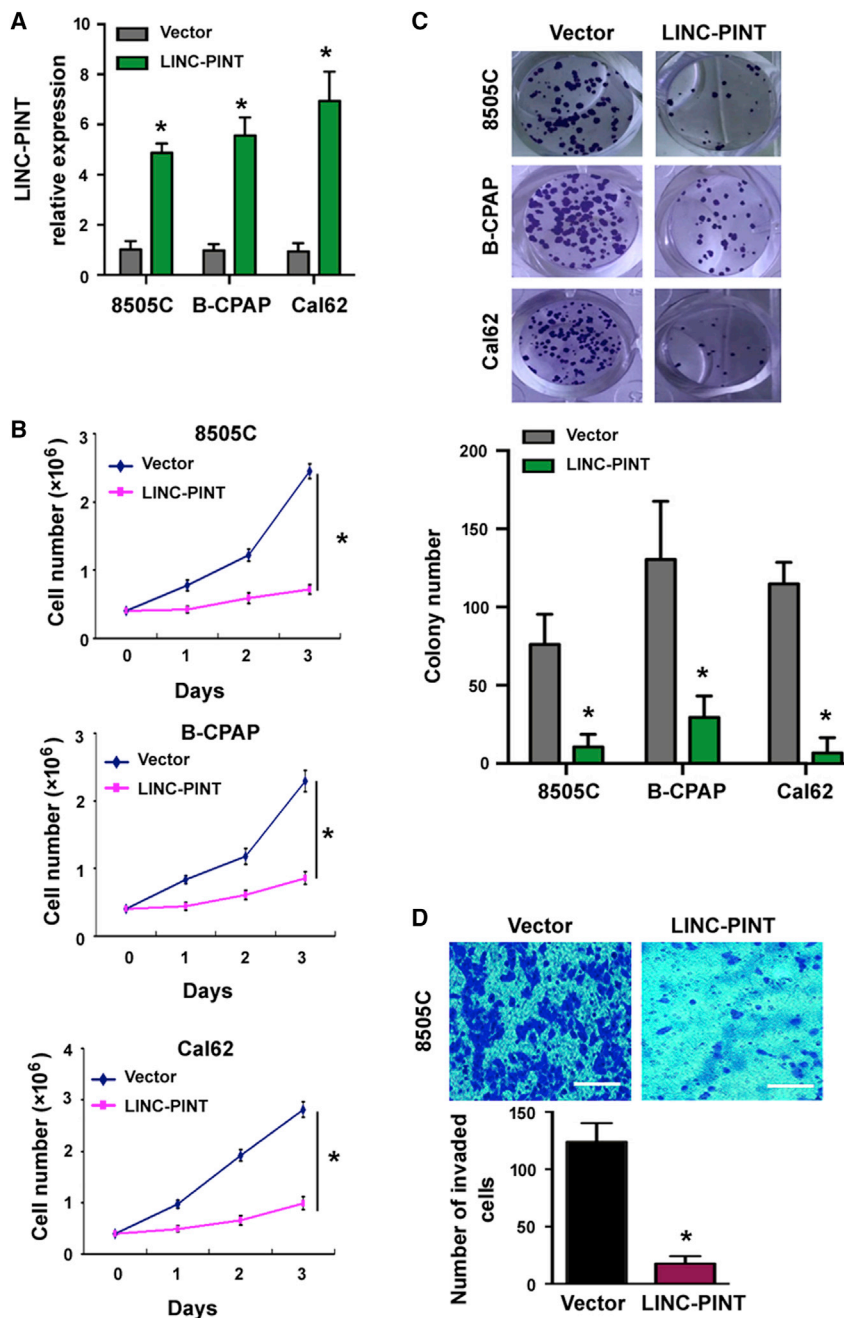


**Figure 2. LINC-PINT Overexpression Suppresses the Proliferation and Invasion of Thyroid Cancer Cells**

(A) Real-time PCR analysis validated the overexpression of LINC-PINT in thyroid cancer cells transfected with LINC-PINT-expressing plasmid. (B) Cell proliferation assay. Cells were counted every day for 3 days. (C) Colony formation assay. Representative images of colonies formed after culturing for 14 days. (D) Invasion capacity of LINC-PINT-overexpressing 8505C cells and control cells assessed using Matrigel-coated Transwell chambers. Representative images of invaded cells after a 24-h incubation. Scale bars, 100  $\mu$ m. \* $p < 0.05$ .

cell proliferation (Figure 5B) and colony formation (Figure 5C) *in vitro* and tumorigenesis (Figure 5D) *in vivo*. In contrast, depletion of miR-767-5p significantly decreased the proliferation (Figure 5E) and invasion (Figure 5F) of 8505C thyroid cancer cells. These results demonstrate that miR-767-5p plays an oncogenic role in thyroid cancer.

#### Repression of TET2 Accounts for the Oncogenic Role of miR-767-5p in Thyroid Cancer Cells

It has been documented that the TET family of genes (TET1, TET2, and TET3) includes potential target genes of miR-767-5p.<sup>19,20</sup> Next, we checked whether miR-767-5p-mediated oncogenic activity in thyroid cancer is ascribed to regulation of TETs. We found that miR-767-5p overexpression led to a selective inhibition of TET2 without affecting the expression of TET1 and TET3 in both 8505C and Cal62 cells (Figure 6A). Overexpression of TET2 (Figure 6B) significantly reversed the effects of miR-767-5p on thyroid cancer cell proliferation (Figure 6C) and invasion (Figure 6D). As a control, TET1 overexpression had no significant impact on miR-767-5p-mediated oncogenic activity (data not shown). In addition, TET2 silencing recapitulated the phenotype of miR-767-5p-overexpressing thyroid cancer cells (Figures 6E–6G). These results collectively suggest that TET2 is the main target gene

involved in miR-767-5p-mediated aggressiveness in thyroid cancer.

was remarkably suppressed by miR-767-5p overexpression (Figures 4E and 4F). Mutation of the miR-767-5p binding site prevented miR-767-5p-mediated inhibition of the LINC-PINT reporter activity. Taken together, these data indicate the functional relationship between miR-767-5p and LINC-PINT in thyroid cancer.

#### miR-767-5p Acts as an Oncogene in Thyroid Cancer

Next, we investigated the function of miR-767-5p in thyroid cancer. Overexpression of miR-767-5p (Figure 5A) significantly promoted

involved in miR-767-5p-mediated aggressiveness in thyroid cancer.

#### LINC-PINT Exerts Suppressive Effects on Thyroid Cancer through the miR-767-5p/TET2 Axis

Analysis of the data from The Cancer Genome Atlas (TCGA) using a web tool Gene Expression Profiling Interactive Analysis (GEPIA; <http://gepia.cancer-pku.cn/>) revealed a positive correlation between LINC-PINT and TET2 expression in thyroid cancer (Figure 7A). Next, we asked whether

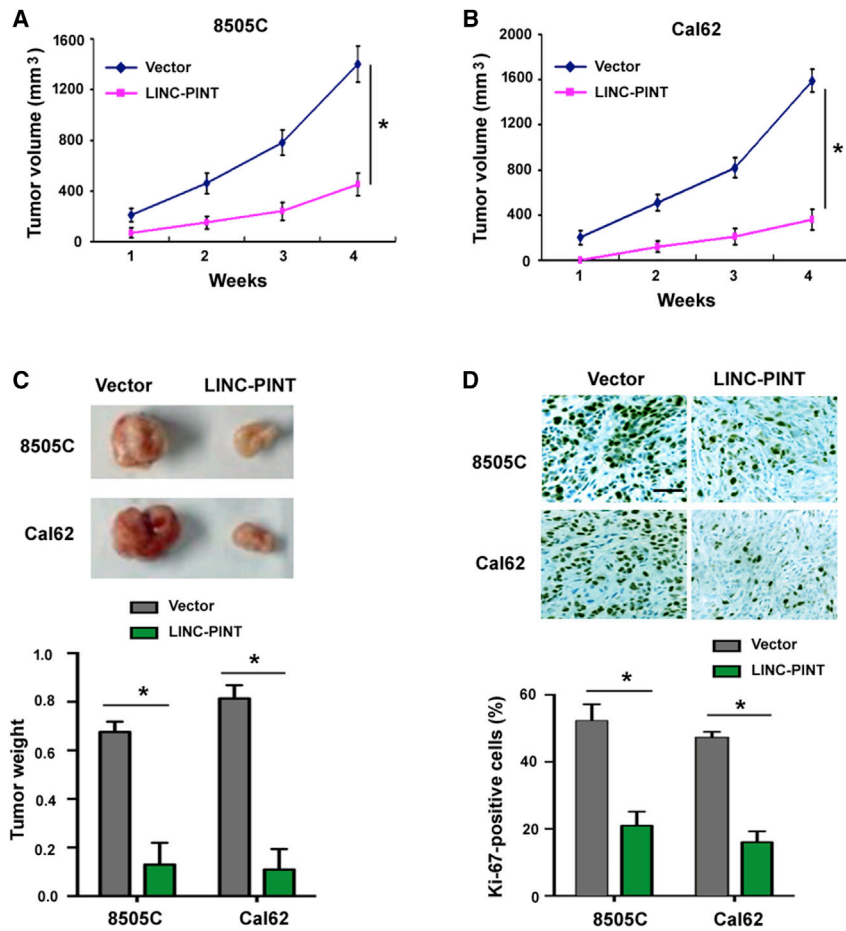


**Figure 3. LINC-PINT Overexpression Retards Tumorigenesis of Thyroid Cancer Cells in Nude Mice**

(A and B) Xenograft growth in nude mice ( $n = 4$  for each group) injected with LINC-PINT-overexpressing (A) 8505C and (B) Cal62 cells and corresponding control cells. (C) Xenograft tumor weight determined 4 weeks after cell injection. Photographs of representative tumors are shown (top). (D) Immunohistochemistry staining of Ki-67 in xenograft tumors. Scale bar, 100  $\mu\text{m}$ . \* $p < 0.05$ .

ues and cell lines have significantly lower levels of LINC-PINT than their normal equivalents. Moreover, the reduction of LINC-PINT is significantly correlated with advanced TNM stage and lymph node metastasis of thyroid cancer patients. These results suggest LINC-PINT as a potential molecular target for the diagnosis and prognosis of thyroid cancer.

Functionally, LINC-PINT acts as a tumor suppressor in thyroid cancer. We found that overexpression of LINC-PINT leads to inhibition of thyroid cancer cell proliferation, colony formation, and invasion. *In vivo* studies confirmed that LINC-PINT overexpression hampers xenograft tumor growth of thyroid cancer cells. The anti-cancer activity of LINC-PINT provides a biological explanation for the clinical findings that LINC-PINT downregulation correlates with aggressive parameters of thyroid cancer.

the miR-767-5p/TET2 axis is implicated in LINC-PINT-mediated suppression of thyroid cancer aggressiveness. We found that the TET2 protein level was higher in the LINC-PINT overexpression group than that in the control group (Figure 7B). However, overexpression of miR-767-5p reversed the elevation of TET2 by LINC-PINT, suggesting that LINC-PINT interferes with the inhibitory effect of miR-767-5p on TET2. Coexpression of miR-767-5p rescued the inhibitory effect of LINC-PINT on cell proliferation (Figure 7C) and invasion (Figure 7D), suggesting that LINC-PINT suppresses the malignant behaviors of thyroid cancer cells by antagonizing miR-767-5p. Next, we tested if LINC-PINT-mediated antitumor activity is dependent on TET2. The results showed that the suppressive effects of LINC-PINT on proliferation and invasion were significantly impaired in TET2-depleted thyroid cancer cells (Figures 7E and 7F). Taken together, LINC-PINT-mediated inhibition of thyroid cancer cell proliferation and invasion is ascribed to antagonization of miR-767-5p and derepression of TET2.

## DISCUSSION

Previous studies have documented that low expression of LINC-PINT has a poor prognostic impact on gastric cancer and pancreatic cancer.<sup>18,21</sup> In the present study, we examined the clinical significance of LINC-PINT in thyroid cancer. Our data show that thyroid cancer tis-

Marín-Béjar et al.<sup>17</sup> suggested that the interaction with polycomb-repressive complex 2 (PRC2) accounts for LINC-PINT-dependent repression of invasion-related gene sets in colon cancer. However, when PRC2 was silenced, LINC-PINT-mediated anticancer activity in thyroid cancer cells was not reversed (data not shown). Therefore, we speculated that a PRC2-independent mechanism is involved in the action of LINC-PINT in thyroid cancer. Given the common interplay between lncRNAs and miRNAs,<sup>15,16</sup> we investigated the key LINC-PINT-associated miRNAs. Of note, we found that LINC-PINT overexpression selectively decreases the expression of miR-767-5p in multiple thyroid cancer cell lines. miR-767-5p is upregulated in thyroid cancer tissues. The Ago2 RIP assay suggests that both miR-767-5p and LINC-PINT are present in the same Ago2 complex. In addition, miR-767-5p is capable of inhibiting the LINC-PINT luciferase reporter activity. These results suggest that LINC-PINT antagonizes both the expression and activity of miR-767-5p in thyroid cancer cells.

Previous studies have revealed that miR-767-5p functions as an oncogene in melanoma and multiple myeloma.<sup>22,23</sup> Consistently, we show that ectopic expression of miR-767-5p significantly augments the

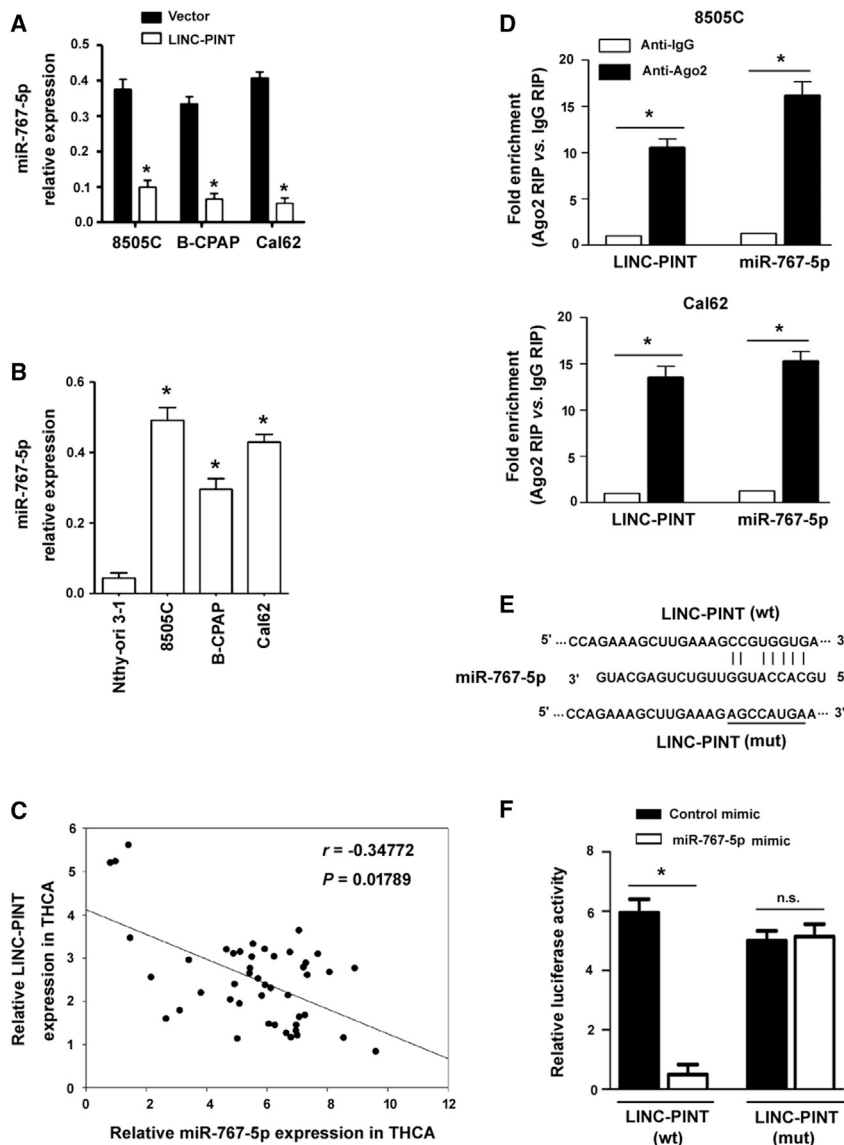


**Figure 4. LINC-PINT Interacts with and Downregulates miR-767-5p**

(A) Effect of LINC-PINT overexpression on the expression of miR-767-5p. \**p* < 0.05 versus vector-transfected cells. (B) Relative expression of miR-767-5p in thyroid cancer cells. \**p* < 0.05 versus Nthy-ori 3-1 cells. (C) Spearman's correlation analysis of the correlation between miR-767-5p and LINC-PINT in thyroid cancer (THCA) tissues (*n* = 46). (D) RIP assay performed with anti-Ago2 antibody in thyroid cancer cells. Immune-precipitated RNA was tested for the abundance of miR-767-5p and LINC-PINT by real-time PCR analysis. \**p* < 0.05. (E) Bioinformatic analysis suggested a putative miR-767-5p binding site in LINC-PINT. The mutation of the binding site was underlined. (F) Dual-luciferase reporter assay. 8505C cells were transfected with miR-767-5p mimic or control miRNA together with wild-type (WT) or mutant (mut) LINC-PINT luciferase reporters. Luciferase activity was measured 48 h later. \**p* < 0.05; n.s., no significance.

the consideration that LINC-PINT and miR-767-5p exert opposite effects on thyroid cancer progression, we hypothesized that LINC-PINT may sponge miR-767-5p to induce the expression of TET2. In line with this hypothesis, we found that LINC-PINT overexpression leads to an increase in TET2 protein levels, which is reversed by miR-767-5p coexpression. TET2 has been documented to play a critical role in tumor progression.<sup>26,27</sup> For instance, Bonvin et al.<sup>26</sup> reported that TET2-dependent epigenetic regulation of downstream genes impairs melanoma initiation and progression. Kunimoto et al.<sup>27</sup> reported that *Tet2* loss and *Nras* mutation cooperatively contribute to myeloid transformation. Therefore, we speculated that derepression of TET2 is required for LINC-PINT-mediated, suppressive effects on thyroid cancer. Indeed, we show that when TET2 is depleted, LINC-PINT-mediated anticancer effects are rescued. Similarly, overexpression of miR-767-5p can restore the aggressive phenotype of LINC-PINT-overexpressing thyroid cancer cells. Taken together, LINC-PINT can downregulate miR-767-5p and antagonize the ability of miR-767-5p to repress TET2 in thyroid cancer cells, consequently blocking cancer cell growth and invasion (Figure 7G).

proliferation and tumorigenesis of thyroid cancer cells. In contrast, knockdown of miR-767-5p restrains thyroid cancer cell proliferation and invasion. Our data point toward a tumor-promoting role for miR-767-5p in thyroid cancer. TET genes have been suggested as potential targets of miR-767-5p.<sup>19,20</sup> Here, we provide evidence that miR-767-5p has the ability to target TET2 in thyroid cancer cells. Depletion of TET2 causes phenotypic changes similar to those seen in miR-767-5p-overexpressing thyroid cancer cells. Rescue studies demonstrate that reconstitution of TET2 expression blocks miR-767-5p-mediated thyroid cancer cell proliferation and invasion. Therefore, an miR-767-5p-mediated aggressive phenotype in thyroid cancer is largely ascribed to downregulation of TET2.

Compelling evidence suggests that lncRNAs can function as a sponge of miRNAs, leading to derepression of miRNA target genes.<sup>24,25</sup> With

In conclusion, our present work highlights the importance of the interplay between LINC-PINT and miR-767-5p in regulating thyroid cancer progression. Downregulation of LINC-PINT is associated with an aggressive phenotype of thyroid cancer. LINC-PINT overexpression sponges miR-767-5p and relieves miR-767-5p-mediated downregulation of TET2, thereby eliciting anticancer effects on thyroid cancer cells. Thus, we suggest the LINC-PINT/miR-767-5p/TET2 axis as a potential therapeutic target for treatment of thyroid cancer.

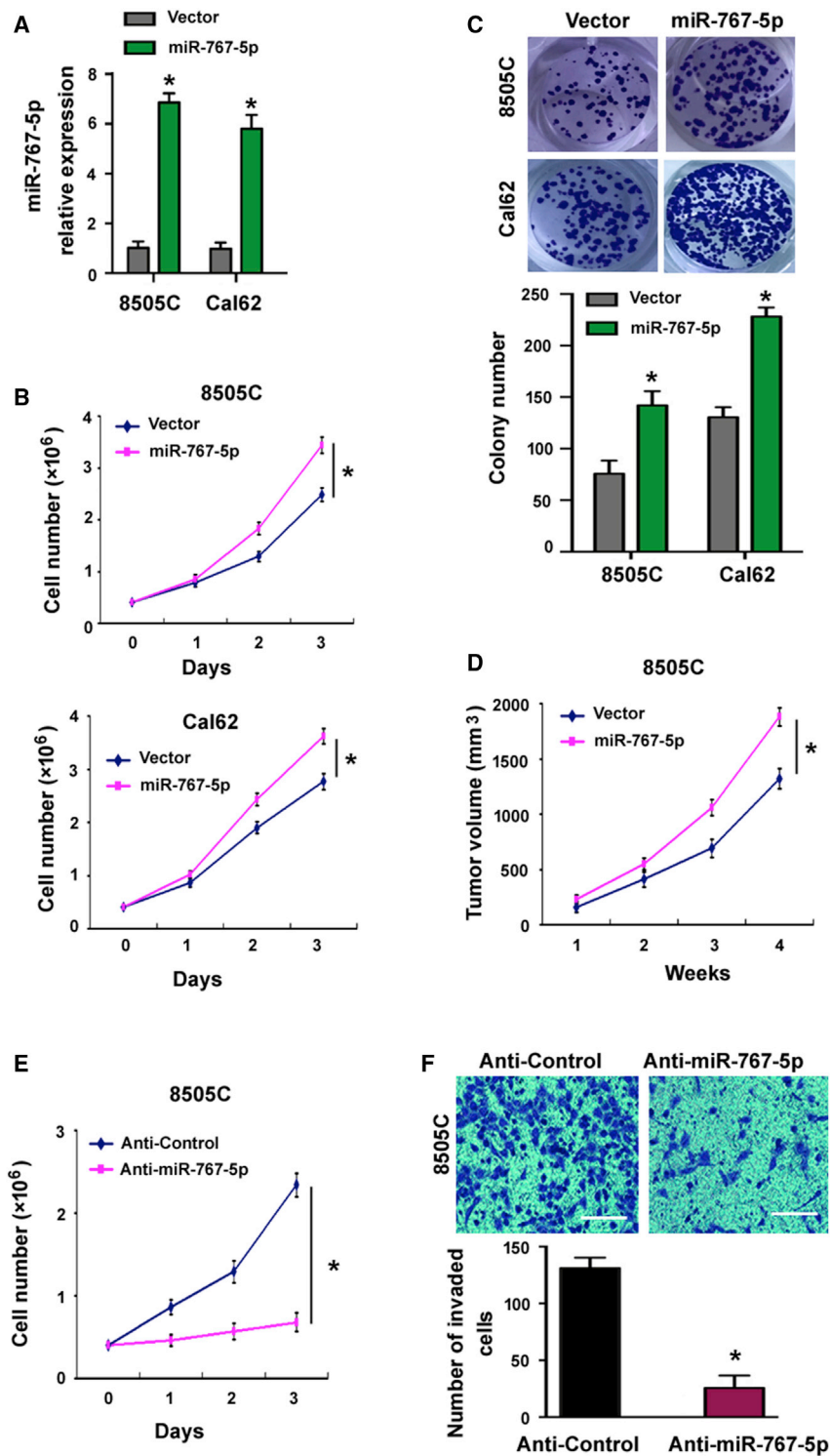


**Figure 5. miR-767-5p Acts as an Oncogene in Thyroid Cancer**

(A) Overexpression of miR-767-5p in thyroid cancer cells transfected with miR-767-5p-expressing plasmid. (B) Cell proliferation assay. Cells were counted every day for 3 days. (C) Colony formation assay. Representative images of colonies formed after culturing for 14 days. (D) Xenograft growth in nude mice ( $n = 4$  for each group) injected with LINC-PINT-overexpressing 8505C and control cells. (E) Cell proliferation assay. Cells transfected with anti-miR-767-5p or anti-control inhibitors were counted every day for 3 days. (F) Invasion capacity of 8505C cells transfected with anti-miR-767-5p or anti-control inhibitors. Representative images of invaded cells after a 24-h incubation. Scale bars, 100  $\mu\text{m}$ . \* $p < 0.05$ .

The First Affiliated Hospital of Zhengzhou University (Zhengzhou, China). Clinicopathological information was retrieved from patient medical records. The cohort of patients included 43 PTC, 9 FTC, 3 ATC, and 5 MTC. Thirty-six patients presented lymph node metastasis. Thirty-one patients were at TNM I and II and 29 at III and IV. No patient received any anticancer treatment before surgery. Surgical specimens were immediately frozen in liquid nitrogen and stored at  $-80^{\circ}\text{C}$  until RNA analysis. Written, informed consent was obtained from each patient. The collection and application of patient specimens were approved by the Human Ethics Committee of The First Affiliated Hospital of Zhengzhou University.

#### Cell Lines

Human thyroid epithelial Nthy-ori 3-1 cells and thyroid cancer cell lines (8505C, B-CPAP, and Cal62) were cultured in RPMI-1640 medium, supplemented with 10% fetal bovine serum (FBS; Invitrogen, Grand Island, NY, USA) in a humidified atmosphere of 5%  $\text{CO}_2$  at  $37^{\circ}\text{C}$ .

#### RNA Isolation and Quantitative Real-Time PCR Analysis

Total RNA was extracted from tissue samples and cell lines using the PureLink RNA Mini Kit (Thermo Fisher Scientific, Waltham, MA, USA). RNA samples were reverse transcribed into cDNA using the Superscript III Reverse Transcriptase Kit (Invitrogen). Quantitative real-time PCR assay was performed using the SYBR Green RT-PCR Kit (TaKaRa, Dalian, China), according

to the manufacturer's protocols. The PCR primers are as follows: LINC-PINT: forward, 5'-GCTTGGCTAGTTGGAGAGTTA-3' and reverse, 5'-CAGACTTTGCTATGTCACAGA-3'; glyceraldehyde 3-phosphate dehydrogenase (GAPDH): forward, 5'-ACCACAGTCC

## MATERIALS AND METHODS

### Patients and Tissue Specimens

A total of 60 tumor samples and adjacent normal tissues were collected from patients with thyroid cancer who underwent surgical resection at

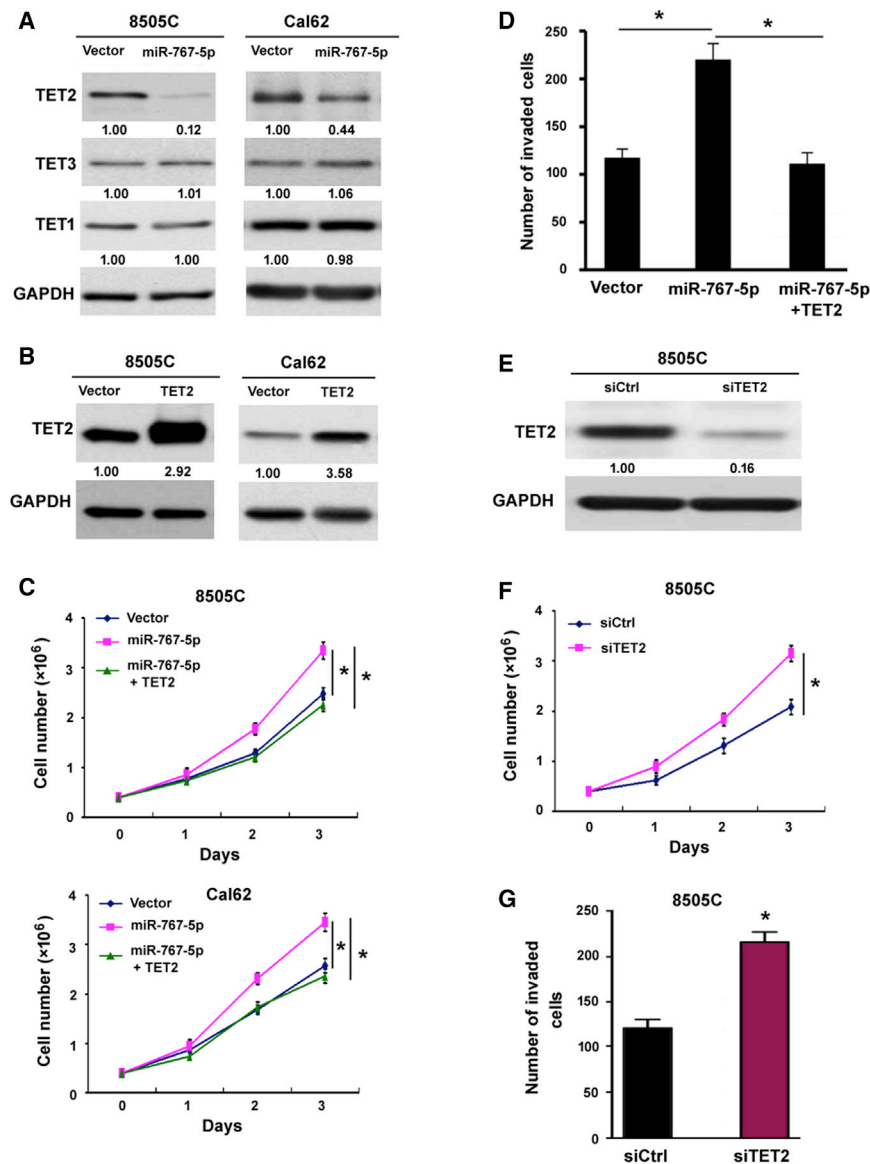


**Figure 6. Repression of TET2 Accounts for the Oncogenic Role of miR-767-5p in Thyroid Cancer Cells**

(A) Western blot analysis of indicated proteins after transfection with miR-767-5p-expressing plasmid or empty vector. Numbers indicate fold change. (B) Western blot analysis of TET2 protein after transfection with TET2-expressing plasmid or empty vector. Numbers indicate fold change. (C) Thyroid cancer cells transfected with indicated constructs were tested for proliferation capacity by direct cell counting. (D) Invasion capacity of 8505C cells transfected with indicated constructs. (E) Western blot analysis of TET2 protein after transfection with control siRNA (siCtrl) or TET2-targeting siRNA (siTET2). Numbers indicate fold change. (F) 8505C cells transfected with siCtrl or siTET2 were tested for proliferation capacity by direct cell counting. (G) Invasion capacity of 8505C cells transfected with siCtrl or siTET2. \* $p < 0.05$ .

GGTGTAAATGGGCTGATAGATGAC-3'. The PCR product was then cloned downstream of the pGL3 firefly luciferase coding sequence. Site-directed mutagenesis was performed using the Site-Directed Mutagenesis Kit (New England Biolabs, Ipswich, MA, USA), according to the manufacturer's protocol. miR-767-5p mimic, anti-miR-767-5p inhibitor, TET2-targeting small interfering RNA (siRNA), and corresponding negative controls were purchased from Sigma-Aldrich (St. Louis, MO, USA).

#### Cell Transfection

Cell transfection was performed using Lipofectamine 3000 (Invitrogen), following the manufacturer's protocol. To generate stable cell lines, transfected cells were selected with G418 (600  $\mu\text{g}/\text{mL}$ ; Sigma-Aldrich) for 2–3 weeks.

#### Cell Proliferation Assay

Cells were seeded into 12-well plates ( $4 \times 10^5$  cells/well) and allowed to grow for 3 days. Cells were counted every day, and growth curves were plotted.

#### Colony Formation Assay

Cells were plated into 6-well plates at a density of 500 cells/well and cultured for 14 days. Colonies were stained with crystal violet and then counted.

#### Transwell Invasion Assay

Transwell invasion assay was performed as described previously.<sup>29</sup> Transwell chambers (8  $\mu\text{m}$  pore size) in a 24-well plate were used this assay.  $1 \times 10^5$  cells suspended in RPMI-1640 medium without FBS were seeded into the upper insert, whereas the lower insert was filled with fresh complete medium containing 10% FBS. After a

ATGCCATCAC-3' and reverse, 5'-ACCACCCTGTTGCTGTA-3'. For the analysis of mature miRNAs, total RNA was reverse transcribed using the miRcute miRNA First-Strand cDNA Synthesis Kit (Tiangen Biotech, Beijing, China) and quantified using the miRcute miRNA qPCR Detection Kit SYBR Green (Tiangen). The relative expression of LINC-PINT and miRNAs was normalized to GAPDH and U6, respectively, and analyzed by the  $2^{-\Delta\Delta\text{CT}}$  method.<sup>28</sup>

#### Plasmids and Oligonucleotides

For gene-overexpression studies, LINC-PINT-, TET2-, and miR-767-5p-expressing DNA fragments were cloned to the pcDNA3.1+ vector. For generation of the LINC-PINT luciferase reporter, the LINC-PINT-expressing fragment was amplified by PCR using the primers: forward, 5'-CTGTGCACCACACTCCTTTC-3' and reverse, 5'-

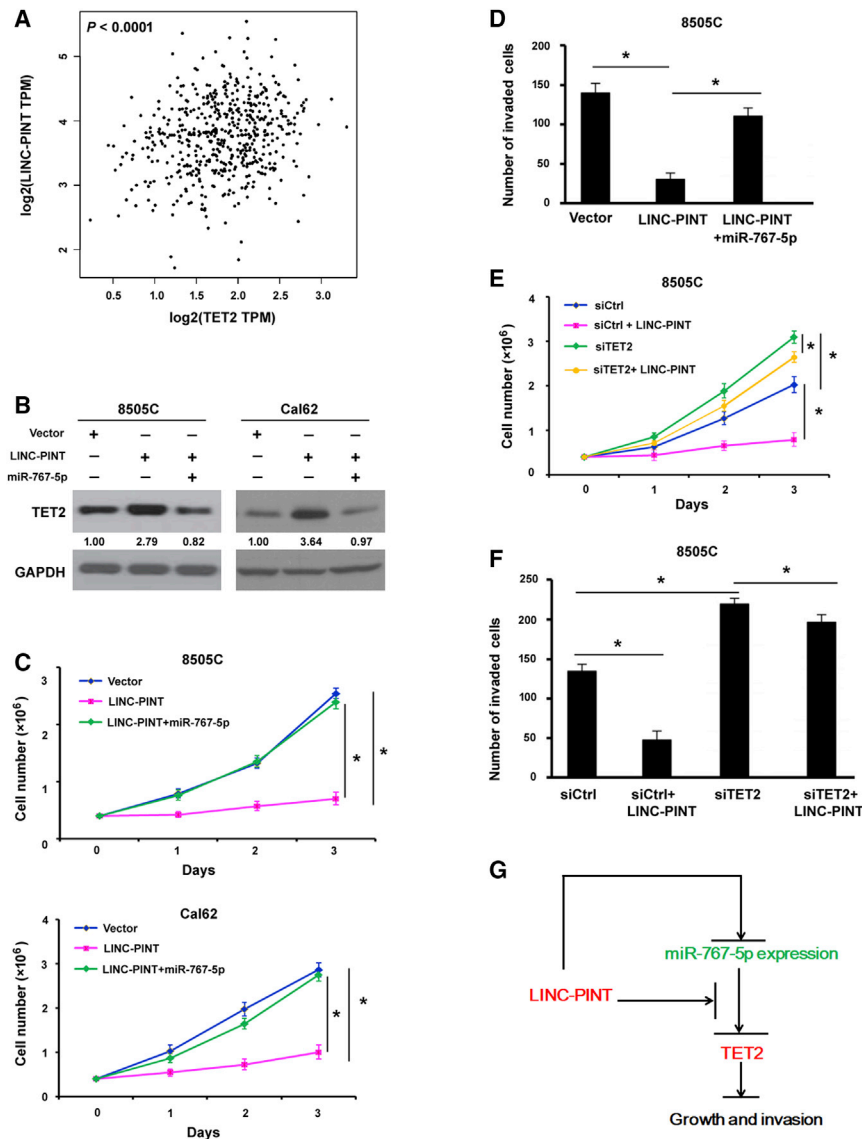


**Figure 7. LINC-PINT Exerts Suppressive Effects on Thyroid Cancer through the miR-767-5p/TET2 Axis**

(A) Analysis of TCGA data suggested a positive correlation between LINC-PINT and TET2 expression in thyroid cancer. (B) Western blot analysis of TET2 protein after transfection with indicated constructs. Numbers indicate fold change. (C) Thyroid cancer cells transfected with indicated constructs were tested for proliferation capacity by direct cell counting. (D) Invasion capacity of 8505C cells transfected with indicated constructs. (E) TET2-depleted and control 8505C cells were transfected, with or without LINC-PINT-expressing plasmid, and tested for proliferation. (F) Analysis of the invasion of 8505C cells transfected with indicated constructs. \* $p < 0.05$ . (G) Schematic model of LINC-PINT function in thyroid cancer growth and invasion. LINC-PINT induces TET2 through suppression of miR-767-5p expression and activity, leading to inhibition of thyroid cancer growth and invasion.

sacrificed after 4 weeks, and tumor weights were recorded. Tumor tissues were processed for immunohistochemistry using anti-Ki-67 antibody (Sigma-Aldrich). Nuclei were counterstained with hematoxylin.

#### RIP Assay

An Ago2-based RIP assay was conducted as described previously.<sup>30</sup> Briefly, cells were suspended in RIP buffer supplemented with protease/RNase inhibitors (Sigma-Aldrich). The cell lysate was mixed with anti-immunoglobulin G (IgG; negative control) or anti-Ago2 antibody (Sigma-Aldrich) conjugated with Protein A/G magnetic beads. The immune-precipitated RNA was purified and subjected to quantitative real-time PCR analysis.

#### Dual-Luciferase Reporter Assay

A luciferase reporter assay was performed as described previously.<sup>29</sup> Briefly, 8505C cells were transfected with miR-767-5p mimic or control miRNA, together with LINC-PINT luciferase reporters (wild type or mutant). After culturing for 48 h, luciferase activity was measured using the Dual Luciferase Reporter Assay Kit (Promega, Madison, WI, USA). *Renilla* luciferase-encoding plasmid was cotransfected to control for transfection efficiency.

#### Western Blot Analysis

Cells were lysated in radioimmunoprecipitation assay lysis buffer supplemented with a protease inhibitor cocktail (Sigma-Aldrich). Protein samples were separated on sodium dodecyl sulfate-polyacrylamide gel electrophoresis and transferred to polyvinylidene difluoride membranes. The membranes were blocked with 5% fat-free milk at room temperature for 2 h, followed by overnight incubation with primary antibodies at 4°C. The primary antibodies included: anti-TET1,

24-h incubation, invade cells were fixed, stained with crystal violet, and counted.

#### Mouse Experiments

All animal experiments were conducted in accordance with national and international guidelines and approved by the Animal Care and Use Institutional Review Board of The First Affiliated Hospital of Zhengzhou University. 6-week-old female BALB/c nude mice were housed in specific pathogen-free conditions on a 12-h light/dark cycle with free access to food and water. Stably transfected 8505C and Cal62 cells were subcutaneously injected into nude mice ( $3 \times 10^6$  cells/mouse). Each group had 4 mice. Tumor size was recorded every week using a caliper. Tumor volumes were calculated based on the following formula: volume =  $(L \times W^2)/2$ , with length (L) being the largest diameter (in millimeters) and width (W) being the smallest diameter (in millimeters). Animals were

anti-TET2, anti-TET3, and anti-GAPDH (all from Novus Biologicals, Littleton, CO, USA). The membranes were then incubated with secondary antibodies (Cell Signaling Technology, Waltham, MA, USA). Signals were visualized using the Pierce Enhanced Chemiluminescence (ECL) Western Blotting Substrate (Thermo Fisher Scientific, Rockford, IL, USA).

### Statistical Analysis

Data are presented as the mean  $\pm$  standard deviation (SD) and analyzed by the Student's *t* test or one-way analysis of variance with Tukey post hoc test. The difference in LINC-PINT expression between thyroid cancer and adjacent normal tissues was determined using the Mann-Whitney *U* test. The chi-square test was used to analyze the relationship between LINC-PINT expression and clinicopathologic parameters of thyroid cancer. The correlation between LINC-PINT and miR-767-5p expression was assessed with Spearman's correlation analysis. A value of  $p < 0.05$  was considered statistically significant.

### SUPPLEMENTAL INFORMATION

Supplemental Information can be found online at <https://doi.org/10.1016/j.omtn.2020.05.033>.

### AUTHOR CONTRIBUTIONS

M.J., J.W., and X.L. designed the experiments and analyzed data. M.J., Z.L., M.P., and M.T. performed the experiments. M.J. wrote the manuscript. All authors reviewed and approved the final manuscript.

### CONFLICTS OF INTEREST

The authors declare no competing interests.

### ACKNOWLEDGMENTS

This work was supported by the Key Scientific and Technological Project of Henan Province (172102310390) and the Key Scientific Research Projects of Colleges & Universities (17A320030).

### REFERENCES

- Cabanillas, M.E., McFadden, D.G., and Durante, C. (2016). Thyroid cancer. *Lancet* 388, 2783–2795.
- Yan, H., Winchester, D.J., Prinz, R.A., Wang, C.H., Nakazato, Y., and Moo-Young, T.A. (2018). Differences in the Impact of Age on Mortality in Well-Differentiated Thyroid Cancer. *Ann. Surg. Oncol.* 25, 3193–3199.
- Seib, C.D., and Sosa, J.A. (2019). Evolving Understanding of the Epidemiology of Thyroid Cancer. *Endocrinol. Metab. Clin. North Am.* 48, 23–35.
- Lee, J.J., Wang, T.Y., Liu, C.L., Chien, M.N., Chen, M.J., Hsu, Y.C., Leung, C.H., and Cheng, S.P. (2017). Dipeptidyl Peptidase IV as a Prognostic Marker and Therapeutic Target in Papillary Thyroid Carcinoma. *J. Clin. Endocrinol. Metab.* 102, 2930–2940.
- Liu, Y., Gunda, V., Zhu, X., Xu, X., Wu, J., Askhatova, D., Farokhzad, O.C., Parangi, S., and Shi, J. (2016). Theranostic near-infrared fluorescent nanoplatforam for imaging and systemic siRNA delivery to metastatic anaplastic thyroid cancer. *Proc. Natl. Acad. Sci. USA* 113, 7750–7755.
- Lan, Y., Pan, H., Li, C., Banks, K.M., Sam, J., Ding, B., Elemento, O., Goll, M.G., and Evans, T. (2019). TETs Regulate Proepicardial Cell Migration through Extracellular Matrix Organization during Zebrafish Cardiogenesis. *Cell Rep.* 26, 720–732.e4.
- Verma, N., Pan, H., Doré, L.C., Shukla, A., Li, Q.V., Pelham-Webb, B., Teijeiro, V., González, F., Krivtsov, A., Chang, C.J., et al. (2018). TET proteins safeguard bivalent promoters from de novo methylation in human embryonic stem cells. *Nat. Genet.* 50, 83–95.
- Collignon, E., Canale, A., Al Wardi, C., Bizet, M., Calonne, E., Dedeurwaerder, S., Garaud, S., Naveaux, C., Barham, W., Wilson, A., et al. (2018). Immunity drives *TET1* regulation in cancer through NF- $\kappa$ B. *Sci. Adv.* 4, eaap7309.
- Zhou, Z., Zhang, H.S., Liu, Y., Zhang, Z.G., Du, G.Y., Li, H., Yu, X.Y., and Huang, Y.H. (2018). Loss of *TET1* facilitates DLD1 colon cancer cell migration via H3K27me3-mediated down-regulation of E-cadherin. *J. Cell. Physiol.* 233, 1359–1369.
- Pitt, S.C., Hernandez, R.A., Nehs, M.A., Gawande, A.A., Moore, F.D., Jr., Ruan, D.T., and Cho, N.L. (2016). Identification of Novel Oncogenic Mutations in Thyroid Cancer. *J. Am. Coll. Surg.* 222, 1036–1043.e2.
- Klinge, C.M. (2018). Non-coding RNAs: long non-coding RNAs and microRNAs in endocrine-related cancers. *Endocr. Relat. Cancer* 25, R259–R282.
- Saeedi Borujeni, M.J., Esfandiary, E., Baradaran, A., Valiani, A., Ghanadian, M., Codoñer-Franch, P., Basirat, R., Alonso-Iglesias, E., Mirzaei, H., and Yazdani, A. (2019). Molecular aspects of pancreatic  $\beta$ -cell dysfunction: Oxidative stress, microRNA, and long noncoding RNA. *J. Cell. Physiol.* 234, 8411–8425.
- Yarani, R., Mirza, A.H., Kaur, S., and Pociot, F. (2018). The emerging role of lncRNAs in inflammatory bowel disease. *Exp. Mol. Med.* 50, 1–14.
- Zhang, X., Liu, L., Deng, X., Li, D., Cai, H., Ma, Y., Jia, C., Wu, B., Fan, Y., and Lv, Z. (2019). MicroRNA 483-3p targets *Pard3* to potentiate TGF- $\beta$ 1-induced cell migration, invasion, and epithelial-mesenchymal transition in anaplastic thyroid cancer cells. *Oncogene* 38, 699–715.
- Wang, Y., Zeng, X., Wang, N., Zhao, W., Zhang, X., Teng, S., Zhang, Y., and Lu, Z. (2018). Long noncoding RNA *DANCR*, working as a competitive endogenous RNA, promotes *ROCK1*-mediated proliferation and metastasis via decoying of miR-335-5p and miR-1972 in osteosarcoma. *Mol. Cancer* 17, 89.
- Ding, J., Yeh, C.R., Sun, Y., Lin, C., Chou, J., Ou, Z., Chang, C., Qi, J., and Yeh, S. (2018). Estrogen receptor  $\beta$  promotes renal cell carcinoma progression via regulating lncRNA *HOTAIR*-miR-138/200c/204/217 associated CeRNA network. *Oncogene* 37, 5037–5053.
- Marín-Béjar, O., Mas, A.M., González, J., Martínez, D., Athie, A., Morales, X., Galduroz, M., Raimondi, I., Grossi, E., Guo, S., et al. (2017). The human lncRNA *LINC-PINT* inhibits tumor cell invasion through a highly conserved sequence element. *Genome Biol.* 18, 202.
- Feng, H., Zhang, J., Shi, Y., Wang, L., Zhang, C., and Wu, L. (2019). Long noncoding RNA *LINC-PINT* is inhibited in gastric cancer and predicts poor survival. *J. Cell. Biochem.* 120, 9594–9600.
- Cheng, J., Guo, S., Chen, S., Mastroianni, S.J., Liu, C., D'Alessio, A.C., Hysolli, E., Guo, Y., Yao, H., Megyola, C.M., et al. (2013). An extensive network of *TET2*-targeting MicroRNAs regulates malignant hematopoiesis. *Cell Rep.* 5, 471–481.
- Loriot, A., Van Tongelen, A., Blanco, J., Klaessens, S., Cannuyer, J., van Baren, N., Decottignies, A., and De Smet, C. (2014). A novel cancer-germline transcript carrying pro-metastatic miR-105 and *TET*-targeting miR-767 induced by DNA hypomethylation in tumors. *Epigenetics* 9, 1163–1171.
- Li, L., Zhang, G.Q., Chen, H., Zhao, Z.J., Chen, H.Z., Liu, H., Wang, G., Jia, Y.H., Pan, S.H., Kong, R., et al. (2016). Plasma and tumor levels of *Linc-pint* are diagnostic and prognostic biomarkers for pancreatic cancer. *Oncotarget* 7, 71773–71781.
- Zhang, K., and Guo, L. (2018). MiR-767 promoted cell proliferation in human melanoma by suppressing *CYLD* expression. *Gene* 641, 272–278.
- Feng, Y., Zhang, L., Wu, J., Khadka, B., Fang, Z., Gu, J., Tang, B., Xiao, R., Pan, G., and Liu, J. (2019). CircRNA *circ\_0000190* inhibits the progression of multiple myeloma through modulating miR-767-5p/MAPK4 pathway. *J. Exp. Clin. Cancer Res.* 38, 54.
- Liu, B., Pan, S., Xiao, Y., Liu, Q., Xu, J., and Jia, L. (2018). *LINC01296/miR-26a/GALNT3* axis contributes to colorectal cancer progression by regulating O-glycosylated *MUC1* via PI3K/AKT pathway. *J. Exp. Clin. Cancer Res.* 37, 316.
- Witkos, T.M., Krzyzosiak, W.J., Fiszler, A., and Koscińska, E. (2018). A potential role of extended simple sequence repeats in competing endogenous RNA crosstalk. *RNA Biol.* 15, 1399–1409.
- Bonvin, E., Radaelli, E., Bizet, M., Luciani, F., Calonne, E., Putmans, P., Nittner, D., Singh, N.K., Santagostino, S.F., Petit, V., et al. (2019). *TET2*-Dependent Hydroxymethylome Plasticity Reduces Melanoma Initiation and Progression. *Cancer Res.* 79, 482–494.

27. Kunitomo, H., Meydan, C., Nazir, A., Whitfield, J., Shank, K., Rapaport, F., Maher, R., Pronier, E., Meyer, S.C., Garrett-Bakelman, F.E., et al. (2018). Cooperative Epigenetic Remodeling by TET2 Loss and NRAS Mutation Drives Myeloid Transformation and MEK Inhibitor Sensitivity. *Cancer Cell* 33, 44–59.e8.
28. Livak, K.J., and Schmittgen, T.D. (2001). Analysis of relative gene expression data using real-time quantitative PCR and the 2(–Delta Delta C(T)) Method. *Methods* 25, 402–408.
29. Jia, M., Shi, Y., Li, Z., Lu, X., and Wang, J. (2019). MicroRNA-146b-5p as an oncomiR promotes papillary thyroid carcinoma development by targeting CCDC6. *Cancer Lett.* 443, 145–156.
30. Chen, S., Chen, J.Z., Zhang, J.Q., Chen, H.X., Qiu, F.N., Yan, M.L., Tian, Y.F., Peng, C.H., Shen, B.Y., Chen, Y.L., and Wang, Y.D. (2019). Silencing of long noncoding RNA LINC00958 prevents tumor initiation of pancreatic cancer by acting as a sponge of microRNA-330-5p to down-regulate PAX8. *Cancer Lett.* 446, 49–61.